

Are Patient-Specific Joint and Inertial Parameters Necessary for Accurate Inverse Dynamics Analyses of Gait?

Jeffrey A. Reinbolt, Raphael T. Haftka, Terese L. Chmielewski, and Benjamin J. Fregly*

Abstract—Variations in joint parameter (JP) values (axis positions and orientations in body segments) and inertial parameter (IP) values (segment masses, mass centers, and moments of inertia) as well as kinematic noise alter the results of inverse dynamics analyses of gait. Three-dimensional linkage models with joint constraints have been proposed as one way to minimize the effects of noisy kinematic data. Such models can also be used to perform gait optimizations to predict post-treatment function given pre-treatment gait data. This study evaluates whether accurate patient-specific JP and IP values are needed in three-dimensional linkage models to produce accurate inverse dynamics results for gait. The study was performed in two stages. First, we used optimization analyses to evaluate whether patient-specific JP and IP values can be calibrated accurately from noisy kinematic data, and second, we used Monte Carlo analyses to evaluate how errors in JP and IP values affect inverse dynamics calculations. Both stages were performed using a dynamic, 27 degrees-of-freedom, full-body linkage model and synthetic (i.e., computer generated) gait data corresponding to a nominal experimental gait motion. In general, JP but not IP values could be found accurately from noisy kinematic data. Root-mean-square (RMS) errors were 3° and 4 mm for JP values and 1 kg, 22 mm, and 74 500 kg * mm² for IP values. Furthermore, errors in JP but not IP values had a significant effect on calculated lower-extremity inverse dynamics joint torques. The worst RMS torque error averaged 4% bodyweight * height (BW * H) due to JP variations but less than 0.25% (BW * H) due to IP variations. These results suggest that inverse dynamics analyses of gait utilizing linkage models with joint constraints should calibrate the model's JP values to obtain accurate joint torques.

Index Terms—Body segment parameters, gait, inverse dynamics, joint parameters, linkage models.

I. INTRODUCTION

ONE of the most valuable biomechanical variables to have for the assessment of any human movement is the time history of the moments of force at each joint" [1]. There are countless applications involving the investigation of human movement ranging from sports medicine to pathological gait. In all cases, the net torque at a particular joint is the result of several factors: muscle forces, muscle moment arms, ligament forces, contact forces due to articular surface geometry, positions and orientations of axes of rotation, and inertial properties of body segments. Assuming that ligament forces are insignificant and that articular contact forces act through the joint center leads to the common simplification that muscles generate the entire joint torque [2]. Individual muscle forces can then be estimated from resultant joint torques computed by inverse dynamics analyses. In the end, inverse dynamics computations depend upon the chosen model parameters, namely body segmental joint parameters (JPs) (joint positions and orientations) and inertial parameters (IPs) (masses, mass centers, and moments of inertia). If the specified parameter values do not match the patient's anatomy and mass distribution, then the predicted gait motions and loads may not be indicative of the clinical situation.

The literature contains a variety of methods to estimate JP and IP values on a patient-specific basis. Anatomic landmark methods estimate parameter values using scaling rules developed from cadaver studies [3]–[6]. In contrast, optimization methods adjust parameter values to minimize errors between model predictions and experimental measurements. Optimizations identifying JP values for 3-D multijoint kinematic models have a high computational cost [7], [8]. Optimizations identifying IP values, but not JP values, have been performed with limited success for planar models of running, jumping, and kicking motions [9].

The literature also contains a variety of studies investigating the sensitivity of inverse dynamics torques to JP and IP values. Challis and Kerwin [2] analyzed the sensitivity of two elbow joint torques to variations in JP and IP values. They used variations consistent with their estimated uncertainties of 10 mm for joint centers and 10% for inertial properties. Holden and Stanhope [10] evaluated the sensitivity of the knee flexion-extension torque to changes in knee center location for multiple walking

Manuscript received September 14, 2006; revised October 15, 2006. The work of B. J. Fregly was supported in part by the Whitaker Foundation and in part by the National Institutes of Health (NIH) National Library of Medicine under Grant R03 LM07332. *Asterisk indicates corresponding author.*

J. A. Reinbolt was with the Department of Mechanical and Aerospace Engineering, University of Florida, Gainesville, FL 32611 USA. He is now with the Department of Bioengineering, Stanford University, Stanford, CA 94305 USA (e-mail: reinbolt@stanford.edu).

R. T. Haftka is with the Department of Mechanical and Aerospace Engineering, University of Florida, Gainesville, FL 32611 USA (e-mail: haftka@ufl.edu).

T. L. Chmielewski is with the Department of Physical Therapy, University of Florida, Gainesville, FL 32611 USA (e-mail: tchmiele@phhp.ufl.edu).

*B. J. Fregly is with the Department of Mechanical and Aerospace Engineering, the Department of Biomedical Engineering, and the Department of Orthopaedics and Rehabilitation, University of Florida, Gainesville, FL 32611 USA (e-mail: fregly@ufl.edu).

Color versions of one or more of the figures in this paper are available online at <http://ieeexplore.ieee.org>.

Digital Object Identifier 10.1109/TBME.2006.889187

speeds. They chose variations of ± 10 mm in the anterior-posterior direction. Pearsall and Costigan [11] used a planar leg model to study the sensitivity of hip forces and torques to inertial property variations of $\pm 40\%$. In contrast, Stagni *et al.* [12] studied the sensitivity of hip torques to variations in hip joint center location of ± 30 mm. Andrews and Mish [13] analyzed knee forces and torques using a planar harmonic oscillating motion with inertial properties variations of $\pm 5\%$. Directly related to knee torque, Della Croce *et al.* [14] investigated how knee kinematics change when the rotation axes are varied by $\pm 10^\circ$. No studies have investigated how errors in JP and IP values together affect inverse dynamics joint torque calculations for gait performed using three-dimensional linkage models.

This study evaluates whether patient-specific JP and IP values are needed to obtain accurate inverse dynamics results for gait using linkage models with joint constraints. We performed the evaluation using a two-stage process. In the first stage, we used optimization analyses to evaluate whether accurate JP and IP values can be found from noisy kinematic movement data. In the second stage, we used Monte Carlo analyses to evaluate whether accurate JP and IP values are needed to obtain accurate inverse dynamics results for gait. While the first stage calibrates both the configuration and mass distribution of the model segments to a patient's movement data, the second stage determines the effect of the model's structure on internal joint torques. Both stages utilized a 3-D, 27 degrees-of-freedom (DOF), full-body gait model possessing 98 JPs and 84 IPs, along with synthetic (i.e., computer generated) gait and isolated joint motion data.

II. METHODS

A. Linkage Model With Joint Constraints

We used a full-body dynamic linkage model of gait for our investigation [7]. The equations of motion for the 3-D, 27 DOF model (Fig. 1) were derived using the Autolev symbolic manipulation software (OnLine Dynamics, Sunnyvale, CA). Comparable to Anderson and Pandy's [15] model structure, three translational and three rotational DOFs express the movement of the pelvis in a Newtonian reference frame. The remaining 13 segments comprise four open chains branching from the pelvis. The positions and orientations of joint axes within adjacent segment coordinate systems are defined by unique JPs. For example, the knee joint axis is simultaneously established in the femoral and tibial coordinate systems. These parameters are used to designate the geometry of the following joint types: three DOF hip, one DOF knee (with internal reaction torque calculated for abduction), two DOF ankle (nonintersecting axes [16]), three DOF back, two DOF shoulder, and one DOF elbow. Each joint type represents the primary *in vivo* motions of the joint. Anatomic landmark methods were used to estimate nominal values for 6 hip [3], 9 knee [5], and 12 ankle [4] JPs. The segment masses, mass centers, and moments of inertia were described by unique IPs. Anatomic landmark methods were used to estimate nominal values for 7 IPs per segment [6].

Parameters defining the structure of the model were referenced to local (i.e., segment fixed) coordinate systems created using OrthoTrak conventions and a static motion capture trial (Motion Analysis Corporation, Santa Rosa, CA). Markers

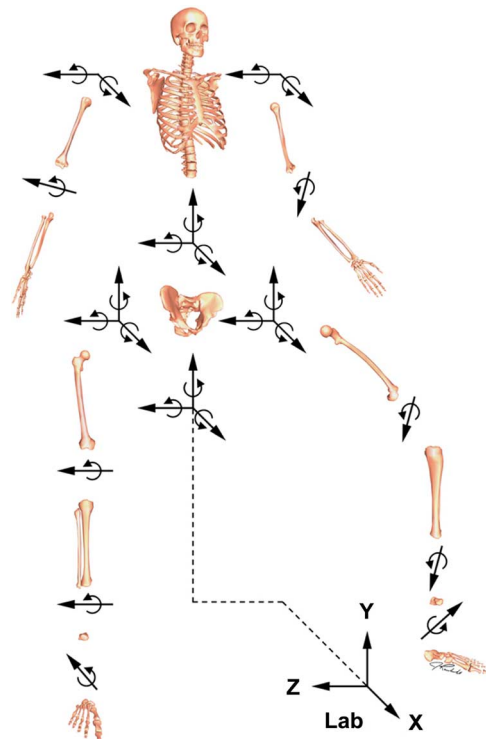


Fig. 1. Schematic of the 3-D, 14 segment, 27 DOF full-body kinematic linkage model with joint constraints.

placed over the left anterior superior iliac spine (ASIS), right ASIS, and superior sacrum were used to define the pelvis segment coordinate system. From percentages of the inter-ASIS distance, a nominal hip joint center location was estimated within the pelvis segment [3]. This nominal joint center served as the origin of the femoral coordinate system, which was subsequently defined using markers placed over the medial and lateral femoral epicondyles. The tibial coordinate system originated at the midpoint of the knee markers and was defined by additional markers located on the medial and lateral malleoli. The talus coordinate system was created according to the conventions of Bogert *et al.* [16], with the longitudinal axis extending along the line perpendicular to both the talocrural and subtalar joint axis. The heel and toe markers, in combination with the tibial superior-inferior axis, defined the foot coordinate system.

B. Experimental and Synthetic Movement Data

Experimental kinematic and kinetic data were collected from a single subject (male, 69.4 kg, 170 cm) using a video-based motion analysis system (Motion Analysis Corporation, Santa Rosa, CA) and two force plates (AMTI, Watertown, MA). Institutional review board approval and informed consent were obtained prior to the experiments. As described above, segment coordinate systems were created from surface marker locations measured during a static standing pose. Unloaded isolated joint motion trials were performed to exercise the primary functional axes of each lower extremity joint (hip, knee, and ankle on each side [7]). For each joint, the subject was instructed to move the distal segment within the physiological range of motion so as to exercise all DOFs of the joint. Three trials were done for

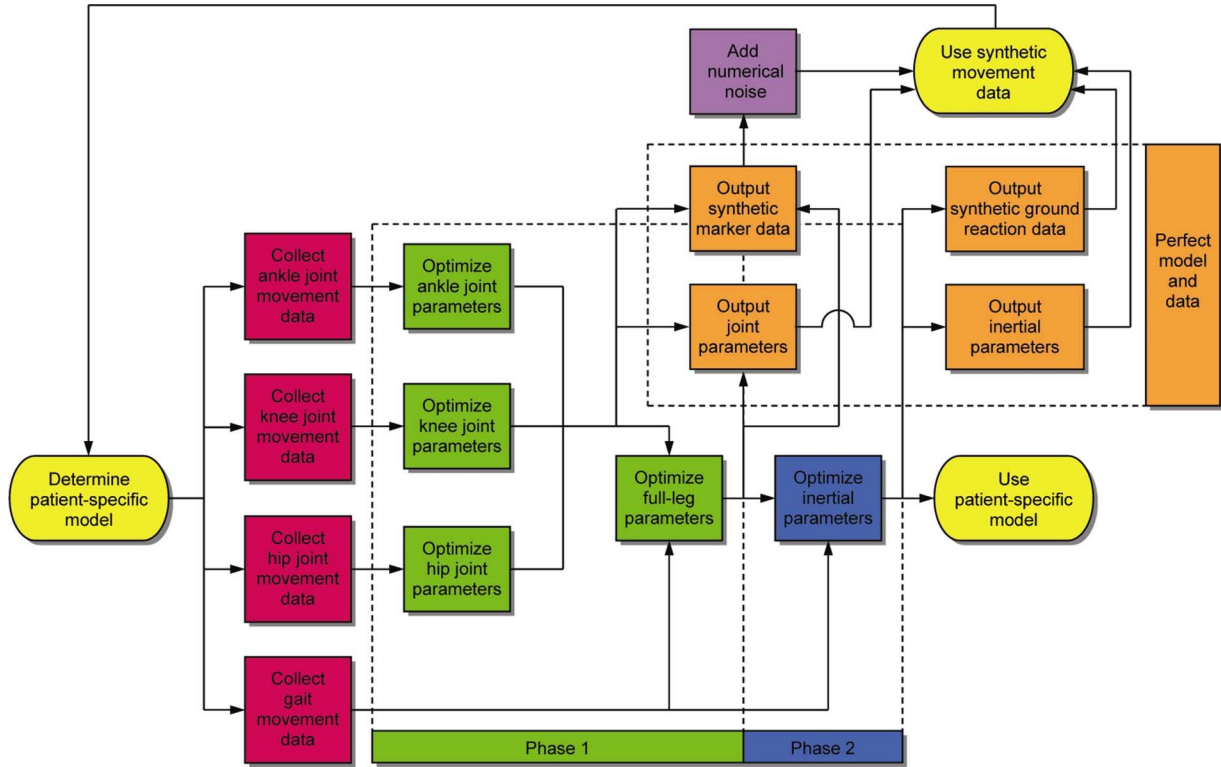


Fig. 2. Flow chart describing the first stage evaluation process using a series of optimization analyses to identify joint (phase 1) and inertial (phase 2) parameter values. To determine a patient-specific model, experimental movement data were collected for isolated joint and full-body gait motions. For phase 1, isolated joint motion data were used to identify JP values for non-weight bearing conditions. Subsequently, gait motion data were used to identify a subset of JP values for weight bearing conditions. For phase 2, optimal JP values and gait motion data were used to identify IP values. In the end, the patient-specific model may be used for dynamic simulations. As a result of the modeling process, known JP and IP values and synthetic motion data comprise a perfect model and data set. To simulate skin and soft tissue movement artifacts, continuous random numerical noise was added to synthetic motion data. The synthetic motion data was used as input data for the two-phase process to evaluate the ability to recover the original marker trajectories and model parameter values.

each joint with all trials performed unloaded. Multiple cycles of standing hip flexion-extension followed by abduction-adduction were recorded. Similar to Leardini *et al.* [17], internal-external rotation of the hip was avoided to reduce skin and soft tissue movement artifacts. Multiple cycles of knee flexion-extension were measured. Finally, multiple cycles of simultaneous ankle plantarflexion-dorsiflexion and inversion-eversion were recorded. Gait motion and ground reaction data were collected to investigate simultaneous motion of all lower extremity joints under load-bearing physiological conditions.

To evaluate the proposed optimization methodology, we generated two types of synthetic movement data from the experimental data sets. The first type was noiseless synthetic data generated by moving the model through motions representative of the isolated joint and gait experiments. By using known JP and IP values and joint motions from the patient, the model with corresponding virtual markers allowed the computation of synthetic marker trajectories and ground reactions that are not contaminated with noise (Fig. 2: perfect model and data). The second type was synthetic data with superimposed numerical noise to simulate skin and soft tissue movement artifacts. The relative movement between skin and underlying bone occurs in a continuous rather than a random fashion [18]. Comparable to the simulated skin movement artifacts of Lu and O'Connor [19], a continuous noise model of the form $A \sin(\omega t + \varphi)$ was

used with the following uniform random parameter values: amplitude ($0 \leq A \leq 1$ cm), frequency ($0 \leq \omega \leq 25$ rad/s), and phase angle ($0 \leq \varphi \leq 2\pi$) [20]. Noise was generated separately for each 3-D coordinate of the marker trajectories and superimposed on the noiseless trajectories.

C. Two-Stage Evaluation Process

We used a two-stage process to evaluate the importance of having accurate patient-specific JP and IP values for obtaining accurate inverse dynamics results of gait. For the first stage, we performed a series of optimization analyses using Matlab's non-linear least squares algorithm (The Mathworks, Natick, MA) to determine how kinematic noise affects our ability to recover known JP and IP values. To evaluate our ability to recover accurate JP values, we performed optimizations that adjusted JP values and model motion to minimize errors between model and experimental (or synthetic) marker locations ((1), Fig. 2: phase 1). For isolated joint motion trials, the design variables were 6 hip, 9 knee, or 12 ankle JP values (\mathbf{p}_{JP}) along with 540 quintic B-spline nodes (\mathbf{q}) parameterizing the generalized coordinate trajectories (20 nodes per DOF [21]). This formulation, which varies JP and motion design variables simultaneously in a single optimization, is different from our previous nested (or two-level) optimization methodology that separated the JP and motion design variables [7], [8]. For the gait trial, the number of

JPs were reduced to 4 hip, 9 knee, and 4 ankle due to inaccuracies in determining joint functional axes with rotations less than 25° [22]. For axes not identified using the gait trial, the JP values were set to the optimal values obtained from the isolated joint trial optimizations. The initial value for each B-spline node and JP value was chosen to be zero to test the robustness of the optimization approach. The JP cost function (e_{JP}) minimized the errors between model (m') and experimental (m) marker locations for each of the three marker coordinates over nm markers and nf time frames

$$e_{JP} = \min_{\mathbf{p}_{JP}, \mathbf{q}} \sum_{i=1}^{nf} \sum_{j=1}^{nm} \sum_{k=1}^3 [m_{ijk} - m'_{ijk}(\mathbf{p}_{JP}, \mathbf{q})]^2. \quad (1)$$

To evaluate our ability to obtain accurate IP values, we performed optimizations that adjusted IP values to minimize the residual forces and torques acting on the 6 DOF ground-to-pelvis joint ((2), Fig. 2: phase 2). Only the gait trial was used in these optimizations. The design variables were a reduced set of 36 IPs (\mathbf{p}_{IP} —7 masses, 8 mass centers, and 21 moments of inertia) accounting for body symmetry and limited joint ranges of motion during gait. The initial seed for each IP value was the nominal value or a randomly altered value within $\pm 50\%$ of nominal. The IP cost function (e_{IP}) utilized a combination of pelvis residual loads (F and T) calculated over all nf time frames and differences between initial (\mathbf{p}'_{IP}) and current (\mathbf{p}_{IP}) IP values. The tracking of initial IP values was necessary to prevent unrealistic results (e.g., negative masses). IP differences were normalized by their respective initial values (\mathbf{p}'_{IP}) to create nondimensional errors. The residual pelvis forces (F) were normalized by body weight (BW) and the residual pelvis torques (T) by body weight times height (BW * H). Once an IP optimization converged, the final IP values were used as the initial guess for a subsequent IP optimization, with this process being repeated until the resulting root-mean-square (RMS) pelvis residual loads converged.

$$e_{IP} = \min_{\mathbf{p}_{IP}} \sum_{i=1}^{nf} \sum_{j=1}^3 \left\{ \left[\frac{F_{ij}(\mathbf{p}_{IP})}{BW} \right]^2 + \left[\frac{T_{ij}(\mathbf{p}_{IP})}{BW * H} \right]^2 \right\} + \left(\frac{\mathbf{p}_{IP} - \mathbf{p}'_{IP}}{\mathbf{p}'_{IP}} \right)^2. \quad (2)$$

The JP and IP optimization procedures were applied to all three data sets (i.e., synthetic data without noise, synthetic data with noise, and experimental data) (Fig. 2). For isolated joint motion trials, JPs for each joint were determined through separate optimizations. For comparison, JPs for all three joints were determined simultaneously for the gait trial. Subsequently, IPs were determined for the gait trial using the previously found optimal JP values. RMS errors between original and recovered parameters, marker distances, and pelvis residual loads were used to quantify the procedure's performance. All optimizations were performed on a 3.4 GHz Pentium 4 PC.

For the second stage, we performed two sets of Monte Carlo analyses to separate the effects of model parameter errors from the effects of kinematic noise on the calculated inverse dynamics joint torques. For the first set, we used synthetic gait

data without noise and variable JP and IP values, while for the second set, we used synthetic gait data with variable noise parameter (NP) amplitude but correct JP and IP values.

The first set of Monte Carlo analyses involved repeated inverse dynamics analyses using variations of JP and IP values, together or separately, within 25%, 50%, 75%, and 100% of their allowable bounds. Each JP and IP value normally found via optimization was selected from a uniform distribution of pseudorandom numbers [23] using bounds consistent with previous studies. Joint center locations were bounded by a maximum of ± 10 mm [2], [10]. Joint axis orientations were bounded by a maximum of $\pm 10^\circ$ [14]. Inertial properties were bounded by a maximum of $\pm 10\%$ of their original values [2]. New model motions were determined by minimizing coordinate errors between model and synthetic marker trajectories [7]. We used 5000 instantiations to ensure convergence of the inverse dynamics torque values. The mean and coefficient of variance ($100 * \text{SD}/\text{mean}$) of all joint torques were within 2% of the final mean and coefficient of variance, respectively, for the last 10% of instantiations [23], [24].

The second set of Monte Carlo analyses involved repeated inverse dynamics analyses using variations of NP values within 25%, 50%, 75%, and 100% of their allowable bounds. The NP values represent the amplitude of simulated skin movement artifacts. The relative movement between skin and underlying bone occurs in a continuous rather than a random fashion [18]. Consequently, we used a previously published continuous noise model of the form $A \sin(\omega t + \varphi)$ with the following uniform random parameter values: amplitude ($0 \leq A \leq 1$ cm), frequency ($0 \leq \omega \leq 25$ rad/s), and phase angle ($0 \leq \varphi \leq 2\pi$) [20]. Noise was generated separately for each 3-D coordinate of the marker trajectories. By finding joint torque and marker distance errors as a function of NP variations, we can use the experimentally determined marker distance errors from the first stage to estimate the joint torque errors that occur experimentally.

For all Monte Carlo analyses, we summarized the distributions of mean inverse dynamics results using boxplots [23]. Each boxplot presented five sample statistics: the minimum (or 10th percentile), the lower quartile (or 25th percentile), the median (or 50th percentile), the upper quartile (or 75th percentile) and the maximum (or 90th percentile). All joint torque and marker distance (i.e., distance between model and synthetic marker locations) error results were reported for the left leg of the model.

III. RESULTS

For the first stage, noisy kinematic data did not limit our ability to determine accurate JP values (Table I). Each JP optimization using noiseless synthetic data precisely recovered the original marker trajectories and model parameters to within an arbitrarily tight convergence tolerance. For the synthetic with noise and experimental data sets, RMS marker distance errors were at most 7 mm (synthetic with noise) and 4 mm (experimental), which are of the same order of magnitude as the amplitude of the continuous noise model. The maximum marker distance errors were 13 mm (synthetic with noise) and 29 mm (experimental), both for the anterior superior iliac spine markers

TABLE I
SUMMARY OF RMS JP AND MARKER DISTANCE ERRORS PRODUCED BY THE PHASE ONE OPTIMIZATIONS AND ANATOMIC LANDMARK METHODS FOR THREE TYPES OF MOVEMENT DATA

Movement data	Method	RMS error	Isolated hip motion	Isolated knee motion	Isolated ankle motion	Combined full-leg motion
Synthetic without Noise	Phase 1 optimization	Marker distances (mm)	9.82e-09	3.58e-08	1.80e-08	2.39e-06
		Orientation parameters (°)	n/a	4.68e-04	6.46e-03	5.45e-03
		Position parameters (mm)	4.85e-05	8.69e-04	6.35e-03	1.37e-02
Synthetic with Noise	Phase 1 optimization	Marker distances (mm)	6.62	5.89	5.43	5.49
		Orientation parameters (°)	n/a	0.09	3.37	3.43
		Position parameters (mm)	0.55	0.59	1.21	3.65
Experimental	Phase 1 optimization	Marker distances (mm)	3.73	1.94	1.43	4.04
	Anatomical landmarks	Marker distances (mm)	4.47	4.03	4.44	6.08

of the pelvis segment during the isolated hip motion trials. JP values found via optimization of synthetic data with noise were close to those (e.g., original anatomic landmark values used to generate synthetic data) found via optimization of synthetic data without noise (Table II). However, for experimental data, JP values found via optimization were markedly different from those found using anatomic landmark methods. Optimizations involving the isolated joint trial data sets (i.e., 1200 time frames of data) required between 108 and 380 seconds of CPU time while the gait trial data set (i.e., 208 time frames of data) required between 70 and 100 seconds of CPU time. These computation times were orders of magnitude faster than those using a previously reported two-level optimization procedure [7].

In contrast, noisy kinematic data was a limiting factor for determining accurate IP values (Table III). Each IP optimization using noiseless synthetic data produced zero pelvis residual loads and recovered the original IP values to within an arbitrarily tight convergence tolerance. For the synthetic with noise and experimental data sets, pelvis residual loads and IP errors remained small, with a random initial seed producing nearly the same pelvis residual loads but slightly higher IP errors than when the correct initial seed was used. IP values found via optimization of synthetic data with noise were different from those (e.g., original anatomic landmark values used to generate synthetic data) found via optimization of synthetic data without noise (Table IV). In contrast, for experimental data, IP values found via optimization were close to those found using anatomic landmark methods. These results are the opposite of what was found for the JPs. Required CPU time ranged from 11 to 48 seconds.

For the second stage, variations in JP values had a large effect on joint torque and marker distance errors while variations in IP values had little effect (Figs. 3 and 4, first three columns). Furthermore, errors due to simultaneous variation of JP and IP

values were no worse than those due to variations in JP values alone, indicating the lack of any significant interaction. For joint torques, RMS errors (Fig. 3) tended to be larger than mean errors (Fig. 4), indicating that the errors were due more to changes in curve shape than in curve offset. For marker distances, RMS and mean errors were of comparable magnitudes.

The influence of JP variations on joint torque errors increased as the inverse dynamics calculations moved proximally (Figs. 3 and 4, first column). For the ankle, joint torque errors were slightly larger for inversion-eversion than for plantarflexion-dorsiflexion. Similarly for the knee, torque errors were slightly larger for abduction-adduction than for flexion-extension. Unlike the other two joints, hip torque errors varied widely with direction, with flexion-extension being much worse than the other two directions. The hip adduction torque errors were unique in that large RMS errors had corresponding small mean errors.

Compared to JP variations, NP variations in the Monte Carlo analyses had only a small effect on joint torque errors and a moderate effect on marker distance errors (Figs. 3 and 4, last column). Both types of errors increased with increasing noise amplitude. For torques, RMS errors (Fig. 3) were larger than mean errors (Fig. 4), while for marker distances, both errors were of comparable magnitude. Though the joint torque errors again increased from distal to proximal, similar to JP variations, the magnitudes of the errors were small.

IV. DISCUSSION

This study evaluated how errors in JP and IP values affect inverse dynamics calculations performed using a gait model with joint constraints and noisy kinematic data. Using optimization and Monte Carlo analyses, we found that first, accurate JP but not IPs could be recovered from noisy kinematic data for joint motion and gait trials, and second, accurate joint but not IPs

TABLE II
DIFFERENCES BETWEEN JPs (I.E., KINEMATIC STRUCTURE PROPERTIES USED TO GENERATE SYNTHETIC DATA) PREDICTED BY ANATOMICAL LANDMARK METHODS AND PHASE ONE OPTIMIZATIONS. BODY SEGMENT INDICATES THE SEGMENT IN WHICH THE ASSOCIATED JP IS FIXED

Joint	Joint parameter	Body segment	Single joint optimization		Full leg optimization	
			Synthetic difference	Experimental difference	Synthetic difference	Experimental difference
Hip	Anterior position (mm)	Pelvis	0.03	21.26	0.53	24.47
	Superior position (mm)	Pelvis	0.51	-23.27	6.86	-8.89
	Lateral position (mm)	Pelvis	-0.94	-12.51	-0.94	-12.51
	Anterior position (mm)	Thigh	0.49	8.88	4.35	27.08
	Superior position (mm)	Thigh	0.47	-25.33	5.55	-11.59
	Lateral position (mm)	Thigh	-0.46	-18.13	-0.46	-18.13
Knee	Frontal plane orientation (°)	Thigh	-0.01	-4.39	-0.33	-7.59
	Transverse plane orientation (°)	Thigh	-0.09	-2.49	-1.08	-3.96
	Frontal plane orientation (°)	Shank	-0.14	-4.42	-0.76	-5.25
	Transverse plane orientation (°)	Shank	-0.03	-1.85	-1.01	-6.23
	Anterior position (mm)	Thigh	-0.74	3.01	2.32	10.97
	Superior position (mm)	Thigh	-0.43	9.33	-6.04	11.07
	Anterior position (mm)	Shank	-0.18	0.52	7.64	7.22
	Superior position (mm)	Shank	-0.53	2.68	-4.49	10.13
Ankle (talocrural)	Lateral position (mm)	Shank	-0.84	-6.79	-1.63	2.67
	Frontal plane orientation (°)	Shank	-4.08	1.04	-0.59	9.58
	Transverse plane orientation (°)	Shank	3.85	-23.89	8.79	-18.12
	Anterior position (mm)	Shank	0.24	4.14	-2.09	-3.29
	Superior position (mm)	Shank	-1.76	-18.29	-2.54	-15.85
Ankle (subtalar)	Lateral position (mm)	Shank	2.03	7.08	2.03	7.08
	Transverse plane orientation (°)	Talus	-5.01	7.70	-5.01	7.70
	Transverse plane orientation (°)	Foot	-0.34	-11.79	-0.34	-11.79
	Sagittal plane orientation (°)	Foot	0.59	-10.66	0.59	-10.66
	Superior position (mm)	Talus	0.78	4.23	0.78	4.23
	Anterior position (mm)	Foot	0.59	-6.05	0.59	-6.05
	Superior position (mm)	Foot	-1.19	-14.85	-1.19	-14.85
Lateral position (mm)	Foot	0.82	3.09	0.82	3.09	

TABLE III
SUMMARY OF RMS IP AND PELVIS RESIDUAL LOAD ERRORS PRODUCED BY THE PHASE TWO OPTIMIZATIONS AND ANATOMIC LANDMARK METHODS FOR THREE TYPES OF MOVEMENT DATA

Movement data	Method	RMS error				
		Force (N)	Torque (N*m)	Inertia (kg*mm ²)	Mass (kg)	Center of mass (mm)
Synthetic without Noise	Phase 2 optimization	8.04e-10	2.16e-10	5.13e-07	1.22e-10	7.11e-10
Synthetic with Noise (correct seed)	Phase 2 optimization	16.92	4.93	5670	1.08	6.64
Synthetic with Noise (random seeds)	Phase 2 optimization	16.96±0.44	5.24±0.23	74,500±18,100	1.33±0.39	21.60±2.92
Experimental	Phase 2 optimization	27.89	12.66	n/a	n/a	n/a
	Anatomical landmarks	34.81	13.75	n/a	n/a	n/a

are needed to obtain accurate inverse dynamics results for gait. These findings are dependent in part on the amplitude and characteristics of the synthetic kinematic noise used in our study. Experimental skin and soft tissue artifacts may be quite different from our simulated noise. Our conclusions may not be

true for ballistic movements involving high accelerations, such as jumping or throwing. Overall, our results suggest that it is worth the time and effort to find patient-specific JP values via optimization, while it is not worth the effort to use optimization to find patient-specific IP values.

TABLE IV
DIFFERENCES BETWEEN IPS (I.E., MASS DISTRIBUTION PROPERTIES USED TO GENERATE SYNTHETIC DATA) PREDICTED BY ANATOMICAL LANDMARK METHODS AND PHASE TWO OPTIMIZATIONS. BODY SEGMENT INDICATES THE SEGMENT IN WHICH THE ASSOCIATED IP IS FIXED

Category	Body segment	Direction	Synthetic differences		Experimental differences
			Correct seed	Random seeds (10 cases)	
Mass (kg)	Pelvis		0.428	0.701±1.87	0.057
	Thigh		1.02	1.45±1.02	-0.829
	Shank		0.269	0.389±0.386	-0.031
	Foot	n/a	0.129	0.162±0.295	0.035
	Head and trunk		-3.38	-3.11±1.34	-0.175
	Upper arm		-0.046	-0.305±0.485	0.005
	Lower arm and hand		0.101	0.215±0.467	0.009
Center of mass (mm)	Pelvis	Anterior	-2.69	-6.51±22.9	0.230
		Superior	0.413	-1.24±5.44	0.012
	Thigh	Superior	3.48	10.1±18.4	9.81
	Shank	Superior	-16.6	-17.3±44.8	-7.65
	Foot	Anterior	-4.83	-10.4±19.0	0.630
		Superior	0	0.007±0.119	0
	Head and trunk	Superior	-24.7	-43.1±13.8	1.66
	Upper arm	Superior	-2.40	-11.5±49.6	0.110
	Lower arm and hand	Superior	-12.900	-4.21±43.6	0.370
	Moment of inertia (kg*mm ²)	Pelvis	Anterior	55.3	-2240±23000
Superior			-111	-2410±18100	-903
Lateral			-121	-2280±16400	-11.9
Thigh		Anterior	2060	-11400±53900	2860
		Superior	-71.4	567±13500	-14.5
		Lateral	-4560	27300±53100	-9060
Shank		Anterior	-99.1	851±11900	-598
		Superior	0.680	-849±1040	1.85
		Lateral	209	-919±6650	415
Foot		Anterior	-0.594	-17.3±645	-0.091
		Superior	-0.086	316±1290	-0.641
		Lateral	3.06	28.7±657	13.6
Head and trunk		Anterior	-33000	-55600±335000	-308000
		Superior	-615	-33700±36200	-2870
		Lateral	-4130	159000±268000	-17300
Upper arm		Anterior	-16.2	-911±5650	-137
		Superior	-0.179	-41.4±1290	-0.940
	Lateral	-0.790	1970±3290	-1.60	
Lower arm and hand	Anterior	-16.3	891±4970	-109	
	Superior	-0.089	-195±502	-0.750	
	Lateral	-58.4	3590±3780	-11.5	

For the first stage of this study, we cannot claim that models fitted with the optimization approach will reproduce the actual functional axes and inertial properties of the patient. The results of the synthetic data with noise, where the RMS errors in the recovered parameter values were not zero, suggest this conclusion. At the same time, the optimized parameter values corresponded to a lower cost function value in each case than did the “correct” parameter values from which the synthetic data were generated. Thus, we can only claim that the optimized model structure provides the best possible fit to the imperfect kinematic data.

A modification to our optimization methodology is the choice of scale factors, or weights, used in the IP optimization

cost function (2). By normalizing residual pelvis torques by the additional height term, 41% less weight is placed on the residual pelvis torques compared to forces. As a result, the reported pelvis residual torque (13 Nm) is relatively large compared to the force (28 N). The cost function has sufficient flexibility to tailor the weights in order to achieve a desired magnitude of residual loads. For example, one may choose to normalize torque values by $BW*$ (pelvic width) to place more importance on torque residuals. We have implemented this scale factors and found little change in the resulting pelvis residual forces (27 N) and torques (12 Nm). By placing more numerical emphasis on the torques, there was a decrease in both residual forces and torques because the tracking of IP

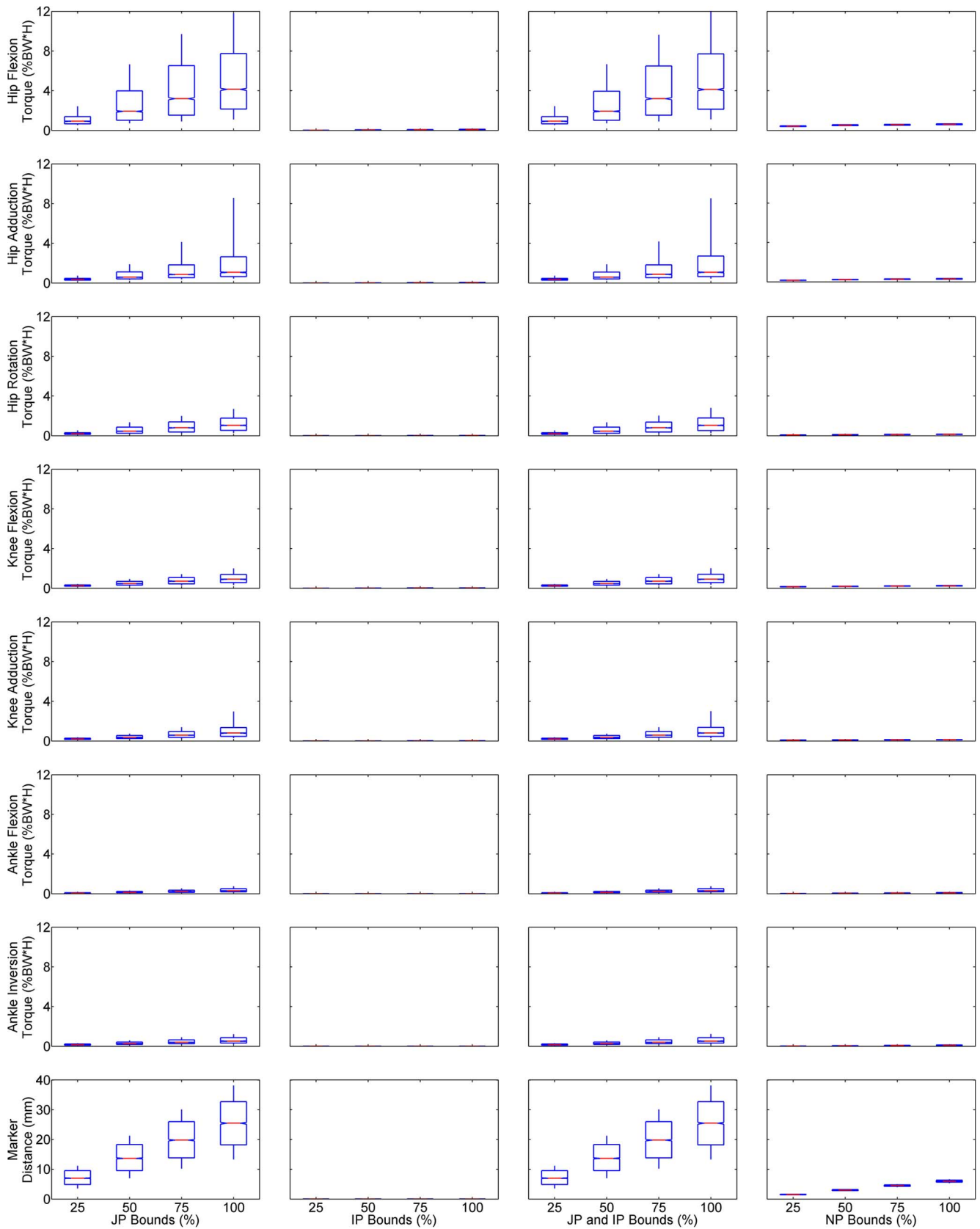


Fig. 3. Boxplots comparing RMS errors in leg joint torques and marker distances. First column contains distributions from varying only JPs. Second column contains distributions from varying only IPs. Third column contains distributions from varying both JPs and IPs. Fourth column contains distributions from varying only the noise amplitude parameter (NP).



Fig. 4. Boxplots comparing mean errors in leg joint torques and marker distances. Columns are the same as in Fig. 3.

parameter values had relatively less importance within the cost function. In the extreme case of scaling residual pelvis torques by BW^* (1 mm), the results were 32 N and 7 Nm for residual

pelvis loads. As one might expect, the weighting of the third term in the cost function also affects final results for the first two terms. Although we have normalized by a certain set of

scale factors (i.e., weights customary for dimensionless kinetic data), a different set of scale factors may be required for a given convergence criteria.

Another modification to our optimization methodology is the addition of a third optimization step that varies JP and IP values simultaneously. We have implemented this approach on the nominal gait data set used in this study. We found that small additional variations in JP and IP values can produce large reductions in residual forces and torques at the pelvis. For the present gait data set, RMS errors in pelvis residual forces and torques fell from 28 to 15 N and 13 to 5 Nm, respectively. These reduced pelvis residual loads are much closer to the synthetic with noise case than before implementation of the third optimization step. This agreement suggests the remaining residuals are due to the adopted approach and kinematic noise rather than rigid body modeling assumptions (e.g., single segment trunk). The third optimization step is reasonable if there is more confidence in the kinetic data compared to the kinematic data. By definition, the JP optimization alone finds the best fit to noisy kinematic data. Understandably, any subsequent changes would mean a lesser fit to the noisy kinematic data. In other words, the kinematic fit is worse in terms of marker distance error, but it may or may not be worse in terms of the true kinematics of the patient. The kinetic data can be used as a supplement to the noisy kinematic data in the fitting process. Caution must be exercised to prevent this third step from overcorrecting JP and IP values to account for incorrect assumptions about model structure.

The JP optimizations determined patient-specific JP values similar to those reported in previous studies. The optimal hip joint center location of 2.94 cm (12.01% posterior), 9.21 cm (37.63% inferior), and 9.09 cm (37.10% lateral) is comparable to 19.30%, 30.40%, and 35.90%, respectively, of the inter-ASIS distance [3]. The optimal femur length (42.23 cm) and tibia length (38.33 cm) are similar to 41.98 cm and 37.74 cm, respectively [6]. The optimal coronal plane rotation (87°) of the talocrural joint correlates to $82.7 \pm 3.7^\circ$ (range 74° to 94°) [5]. The optimal distance (0.58 cm) between the talocrural joint and subtalar joint is analogous to 1.24 ± 0.29 cm [16]. The optimal transverse plane rotation (35°) and sagittal plane rotation (31°) of the subtalar joint are not far outside one standard deviation, but within the recorded ranges, of $23 \pm 11^\circ$ (range 4° to 47°) and $42 \pm 9^\circ$ (range 20.5° to 68.5°), respectively [5]. Compared to anatomic landmark methods reported in the literature, the JP optimization reduced RMS marker distance errors by 17% (hip), 52% (knee), 68% (ankle), and 34% (full leg).

The IP optimization also determined patient-specific IP values that were similar to previous studies. The optimal masses were within an average of 1.99% (range 0.078% to 8.51%), centers of mass within 1.58% (0.047% to 5.84%), and moments of inertia within 0.99% (0.0038% to 5.09%) of the nominal values [6]. Compared to anatomic landmark methods reported in the literature, the IP optimization reduced RMS pelvis residual loads by 20% (forces) and 8% (torques). When JP and IP parameter values were varied simultaneously, the reductions were 57% (forces) and 64% (torques) compared to anatomical landmark methods.

Two conclusions may be drawn from these comparisons. First, the similarities suggest the results are reasonable given the extent of agreement with past studies. Second, the differences between values indicate the extent to which calibration of model parameter values to the patient's movement data via optimization would change their values compared to anatomic landmark methods. Such changes can significantly affect the calculated inverse dynamics joint torques. For example, use of JP values from anatomical landmark rather than optimization methods leads to an RMS knee adduction torque error of more than $0.4 \%BW * H$. In all cases, the JP and IP optimizations successfully reduced cost function values for marker distance errors and pelvis residual loads, respectively, below those resulting from anatomic landmark methods.

For the second stage of this study, the output distributions from the Monte Carlo analyses may have been overestimated. This limitation is the same for any Monte Carlo analysis that assumes parameter independence and uniform distributions. We made these assumptions since we had no prior knowledge of the correlation between or *in vivo* distribution of the various JP and IP values. Consequently, we may have simulated a more diverse assortment of full-body models than would occur in reality. Given the true parameter correlations and distributions, the reported errors would only be reduced. Our results therefore provide a conservative estimate of which categories of parameters are important to calibrate for obtaining accurate joint torques.

Our Monte Carlo results also depend on the selected parameter value bounds. We chose bounds consistent with previous studies [2], [10], [14]. Understandably, the resulting distributions would have been larger if we had used larger JP variations of ± 30 mm [12] and IP variations of $\pm 40\%$ [11]. However, these larger parameter value variations would have been inconsistent with the parameter value uncertainties determined from our optimization analyses in the first stage (closer to ± 10 mm and $\pm 10\%$), making it difficult to combine results from our two stages to approximate joint torque errors that occur experimentally. In addition, using $\pm 40\%$ variations in IP values, Pearsall and Costigan [11] reported small absolute changes (generally less than 0.05 Nm/kg) for joint torques. These changes may be smaller than the errors due to marker placement, skin and soft tissue movement, and equipment accuracy [25]. In the event of an imbalance between JP and IP value ranges, we performed an additional Monte Carlo analysis with IP variations of $\pm 50\%$. For this case, the largest mean RMS error for hip flexion torque increased to a magnitude of $0.31 \%BW * H$ (or $0.53 \%BW$), which corresponds well with Pearsall and Costigan's [11] results of less than 1 %BW. Even for extremely large ranges, IP variations have little influence on calculated joint torques during gait.

Noise parameter value variations in the Monte Carlo analyses did not have as large an influence on calculated joint torques as expected. There are two possible explanations for this finding. First, given that the correct JP values were used, noise added to the synthetic marker coordinate data had a limited effect on the model pose for any particular time frame. Moreover, by optimizing the model motion over all time frames simultaneously, our procedure smoothes out the effects of kinematic noise.

These observations were a motivating factor for using a linkage model with joint constraints to analyze noisy kinematic data [19]. Second, nominal joint torque data for error analysis was generated by a linkage model consistent with our model's joint definitions. However, we do not expect our results to change significantly if small secondary motions were added to the joints, since our optimization approach minimizes secondary motions away from the primary functional axes, similar to a principal component analysis.

The Monte Carlo analyses determined joint torque errors consistent with sensitivity results of previous studies. The hip flexion-extension torque showed the largest RMS error (mean 4.14 % bodyweight * height (BW * H)) comparable to the propagated error mean of 1.29 to 1.57 %BW * H from Stagni *et al.* [12]. The hip abduction-adduction torque had the second largest RMS error (mean 1.06 %BW * H) analogous to the propagated error mean of 1.28 to 1.48 %BW * H from Stagni *et al.* [12]. The knee flexion-extension torque mean RMS error of 0.92 %BW * H is similar to the peak 0.71 %BW * H reported by Holden and Stanhope [10]. Pearsall and Costigan [11] found IP value variations affected joint torques by less than 1 %BW (equivalent to 0.59 %BW * H for our subject), which corresponds to our results.

There are several differences between our Monte Carlo analyses and other sensitivity studies involving JPs and IPs for inverse dynamics analyses. One study [2] separately evaluated both JPs and IPs, while others examined either JPs [10], [12], [14] or IPs [11], [13], [26], [27]. Our study assessed the contribution of JPs and IPs both together and separately. The current work investigated sensitivities during gait, but Challis and Kerwin [2] used an elbow flexion motion. Although some studies [2], [10], [12] considered a localized body region or single joint, this study included a multijoint linkage model of the entire body. None of the above mentioned studies performed Monte Carlo analyses to determine sensitivities of joint torques to JP and IP values.

The Monte Carlo results can be used to estimate the magnitude of joint torque errors one might expect to observe experimentally. Joint torque errors are caused primarily by modeling errors (and in particular JP errors) and kinematic noise. From analysis of experimental gait data in the first stage, RMS marker distance errors can be as low as 4 mm using optimized JPs and 6 mm using JPs from anatomical landmark methods. In a previous study using lower quality kinematic data, we obtained RMS marker distance errors of 8 mm and 14 mm, respectively, using similar approaches. Based on the Monte Carlo results (Fig. 3), 4 mm of marker distance error corresponds to less than 25% variation in JP values and 50% variation in NP amplitude, while 14 mm of error corresponds to 50% variation in JP values and more than 100% variation in NP amplitude. By adding the corresponding torque errors from the appropriate JP and NP columns, one can estimate the total torque error for a particular situation. For example, for our current gait data with only 4 mm of RMS marker distance error, the RMS error in the knee adduction torque was less than 0.1 %BW * H.

The physical significance of our findings is of relevance to clinical and experimental biomechanists. For example, if the model does not match the patient, then the inverse and forward

dynamic simulation results may not be representative of the clinical situation. Understandably, a model constructed of rigid links within a multilink chain and simple mechanical approximations of joints will not precisely match a patient's anatomy and function. However, the best possible agreement to experimental motion data should be made within the bounds of the chosen dynamic model. Within the context of our study, the accuracy of dynamic analyses made for a particular patient is determined in part by the fitness of the JP and IP values. Without expensive medical images, model parameter values are typically estimated from external landmarks that have been identified in previous studies. The estimated values may be improved by formulating an optimization problem using motion-capture data. By using a multiphase optimization technique, researchers may build more accurate biomechanical models of the individual human structure. As a result, the optimal models will provide reliable foundations for future patient-specific dynamic analyses and optimizations of gait.

REFERENCES

- [1] D. A. Winter, "Overall principle of lower limb support during stance phase of gait," *J. Biomech.*, vol. 13, no. 11, pp. 923–927, 1980.
- [2] J. H. Challis and D. G. Kerwin, "Quantification of the uncertainties in resultant joint moments computed in a dynamic activity," *J. Sports Sci.*, vol. 14, no. 3, pp. 219–231, 1996.
- [3] A. L. Bell, D. R. Pedersen, and R. A. Brand, "A comparison of the accuracy of several hip center location prediction methods," *J. Biomech.*, vol. 23, no. 6, pp. 617–621, 1990.
- [4] V. T. Inman, *The Joints of the Ankle*. Baltimore, Maryland: Williams and Wilkins Company, 1976.
- [5] D. L. Churchill, S. J. Incavo, C. C. Johnson, and B. D. Beynnon, "The transepicondylar axis approximates the optimal flexion axis of the knee," *Clinical Orthopaedics and Related Research*, vol. 356, no. 1, pp. 111–118, 1998.
- [6] P. de Leva, "Adjustments to Zatsiorsky-Seluyanov's segment inertia parameters," *J. Biomech.*, vol. 29, no. 9, pp. 1223–1230, 1996.
- [7] J. A. Reinbolt, J. F. Schutte, B. J. Fregly, R. T. Haftka, A. D. George, and K. H. Mitchell, "Determination of patient-specific multi-joint kinematic models through two-level optimization," *J. Biomech.*, vol. 38, no. 3, pp. 621–626, 2005.
- [8] I. W. Charlton, P. Tate, P. Smyth, and L. Roren, "Repeatability of an optimized lower body model," *Gait Posture*, vol. 20, no. 2, pp. 213–221, 2004.
- [9] C. L. Vaughan, J. G. Andrews, and J. G. Hay, "Selection of body segment parameters by optimization methods," *J. Biomech. Eng.*, vol. 104, no. 1, pp. 38–44, 1982.
- [10] J. P. Holden and S. J. Stanhope, "The effect of variation in knee center location estimates on net knee joint moments," *Gait Posture*, vol. 7, no. 1, pp. 1–6, 1998.
- [11] D. J. Pearsall and P. A. Costigan, "The effect of segment parameter error on gait analysis results," *Gait Posture*, vol. 9, no. 3, pp. 173–183, 1999.
- [12] R. Stagni, A. Leardini, M. G. Benedetti, A. Cappozzo, and A. Cappello, "Effects of hip joint centre mislocation on gait analysis results," *J. Biomech.*, vol. 33, no. 11, pp. 1479–1487, 2000.
- [13] J. G. Andrews and S. P. Mish, "Methods for investigating the sensitivity of joint resultants to body segment parameter variations," *J. Biomech.*, vol. 29, no. 5, pp. 651–654, 1996.
- [14] U. Della Croce, A. Leardini, C. Lorenzo, and A. Cappozzo, "Human movement analysis using stereophotogrammetry part 4: Assessment of anatomical landmark misplacement and its effects on joint kinematics," *Gait Posture*, vol. 21, no. 2, pp. 226–237, 2005.
- [15] F. C. Anderson and M. G. Pandy, "A dynamic optimization solution for vertical jumping in three dimensions," *Comput. Meth. Biomech. Biomed. Eng.*, vol. 2, no. 3, pp. 201–231, 1999.
- [16] A. J. van den Bogert, G. D. Smith, and B. M. Nigg, "In vivo determination of the anatomical axes of the ankle joint complex: An optimization approach," *J. Biomech.*, vol. 27, no. 12, pp. 1477–1488, 1994.

- [17] A. Leardini, A. Cappozzo, F. Catani, S. Toksvig-Larsen, A. Petitto, V. Sforza, G. Cassanelli, and S. Giannini, "Validation of a functional method for the estimation of hip joint centre location," *J. Biomech.*, vol. 32, no. 1, pp. 99–103, 1999.
- [18] A. Cappozzo, F. Catani, and A. Leardini, "Skin movement artifacts in human movement photogrammetry," in *Proc. XIVth Congr. Int. Soc. Biomechanics*, Paris, France, Jul. 4–8, 1993, pp. 238–239.
- [19] T.-W. Lu and J. J. O'Connor, "Bone position estimation from skin marker coordinates using global optimisation with joint constraints," *J. Biomech.*, vol. 32, no. 2, pp. 129–134, 1999.
- [20] L. Chéze, B. J. Fregly, and J. Dimnet, "A solidification procedure to facilitate kinematic analyses based on video system data," *J. Biomech.*, vol. 28, no. 7, pp. 879–884, 1995.
- [21] C. Mazza and A. Cappozzo, "An optimization algorithm for human joint angle time-history generation using external force data," *Ann. Biomed. Eng.*, vol. 32, no. 5, pp. 765–772, 2004.
- [22] L. Chéze, B. J. Fregly, and J. Dimnet, "Determination of joint functional axes from noisy marker data using the finite helical axis," *Hum. Movement Sci.*, vol. 17, no. 1, pp. 1–15, 1998.
- [23] F. J. Valero-Cuevas, M. E. Johanson, and J. D. Towles, "Towards a realistic biomechanical model of the thumb: The choice of kinematic description may be more critical than the solution method or the variability/uncertainty of musculoskeletal parameters," *J. Biomech.*, vol. 36, no. 7, pp. 1019–1030, 2003.
- [24] G. S. Fishman, *Monte Carlo: Concepts, Algorithms, and Applications*. New York: Springer, 1996.
- [25] K. J. Deluzio, U. P. Wyss, J. Li, and P. A. Costigan, "A procedure to validate three-dimensional motion assessment systems," *J. Biomech.*, vol. 26, no. 6, pp. 753–759, 1993.
- [26] G. Rao, D. Amerantini, E. Berton, and D. Favier, "Influence of body segments' parameters estimation models on inverse dynamics solutions during gait," *J. Biomech.*, 2005, to be published.
- [27] M. P. Silva and J. A. Ambrosio, "Sensitivity of the results produced by the inverse dynamic analysis of a human stride to perturbed input data," *Gait Posture*, vol. 19, no. 1, pp. 35–49, 2004.



Jeffrey A. Reinbolt received the B.S. degree in engineering science, the M.S. degree in biomedical engineering, and the Ph.D. degree in mechanical engineering from the University of Florida, Gainesville, in 1996, 2003, and 2006, respectively.

He is a Distinguished Postdoctoral Fellow at Stanford University, Stanford, CA, where he develops and applies software to study the dynamics and function of human health and disease. His appointment is within the Center for Physics-Based Simulation of Biological Structures, which is one of

seven National Centers for Biomedical Computation supported by the National Institutes of Health Roadmap for Bioinformatics and Computational Biology. From 1996–2001, he was a Clinical Development Specialist for a start-up medical device manufacturer where he performed domestic and international clinical research and product development of a novel robotic system enabling minimally invasive microsurgery. His research interests include: biomedical computation, simulation-based surgical and rehabilitation treatment planning, innovative patient-specific modeling, optimization methods, robotics for minimally invasive surgery, and clinical feasibility studies for medical device development.

Dr. Reinbolt is a member of the American Association for the Advancement of Science sponsored by the AAAS/Science Program for Excellence in Science.

Raphael T. Haftka photograph and biography not available at the time of publication.



Terese L. Chmielewski received the B.S. degree in health science and the M.A. degree in physical therapy from the College of St. Scholastica, Duluth, MN, in 1991 and 1993, respectively. She received the Ph.D. degree in biomechanics and movement sciences from the University of Delaware, Newark, in 2002.

She was a full-time Physical Therapist with HealthSouth Sports Medicine and Rehabilitation, Birmingham, AL, from 1993–1998. She completed a sports physical therapy fellowship at HealthSouth from 1996–1997. In 2002, she joined the Department of Physical Therapy at the University of Florida, Gainesville, and is currently an Assistant Professor. Her research interests are the identification and treatment of neuromuscular impairments after musculoskeletal injury to improve rehabilitation outcomes. She has a particular interest in decreasing the risk of osteoarthritis after knee injury.

Dr. Chmielewski is a member of the American Physical Therapy Association and the American College of Sports Medicine.



Benjamin J. Fregly received the B.S. degree in mechanical engineering from Princeton University, Princeton, NJ, in 1986 and the M.S. and Ph.D. degrees in mechanical engineering from Stanford University, Stanford, CA, in 1987 and 1993, respectively.

He worked as a Post-Doctoral Fellow at the University of Lyon, Lyon, France from 1993 to 1994. From 1995–1999, he worked as a Research and Development Engineer for the Mechanical Division of Parametric Technology Corporation, San Jose, CA.

Since 1999, he has been on the faculty of the Mechanical & Aerospace Engineering and Biomedical Engineering departments at the University of Florida in Gainesville, where he is currently an Associate Professor. His research involves dynamic modeling, simulation, and optimization of the human musculoskeletal system with an emphasis on the development of patient-specific and dynamic contact modeling approaches. Clinical applications include the design of rehabilitation methods, surgical procedures, and joint replacements for treating knee osteoarthritis.

Dr. Fregly was awarded a Faculty Early Career Development (CAREER) Award by the National Science Foundation. He has been a member of the American Society of Mechanical Engineers since 1987 and of the American Society of Biomechanics since 1988 and is currently on the Executive Board of the Technical Group on Computer Simulation for the International Society of Biomechanics.